Journal of Controlled Release 223 (2016) 42–52

Contents lists available at ScienceDirect

Journal of Controlled Release

journal homepage: www.elsevier.com/locate/jconrel

Enhanced FcRn-dependent transepithelial delivery of IgG by Fc-engineering and polymerization

Stian Foss [a,b], Algirdas Grevys [a,b], Kine Marita Knudsen Sand [a,b], Malin Bern [a,b], Pat Blundell [e], Terje E. Michaelsen [c,d], Richard J. Pleass [e], Inger Sandlie [a,b], Jan Terje Andersen [a,b,*]

[a] Centre for Immune Regulation (CIR), Department of Biosciences, University of Oslo, N-0316, Oslo, Norway
[b] Department of Immunology and CIR, Oslo University Hospital, Rikshospitalet, University of Oslo, N-0372, Oslo, Norway
[c] Department of Bacteriology and Immunology, Norwegian Institute of Public Health, Oslo, Norway
[d] Department of Chemical Pharmacy, School of Pharmacy, University of Oslo, Oslo, Norway
[e] Liverpool School of Tropical Medicine, Pembroke Place, Liverpool L3 5QA, UK

ARTICLE INFO

Article history:
Received 24 September 2015
Received in revised form 14 December 2015
Accepted 19 December 2015
Available online 21 December 2015

Keywords:
FcRn
pH-dependent binding
IgG
Fc-fusion
Transcytosis
Epithelial
Mucosal barrier

ABSTRACT

Monoclonal IgG antibodies (Abs) are used extensively in the clinic to treat cancer and autoimmune diseases. In addition, therapeutic proteins are genetically fused to the constant Fc part of IgG. In both cases, the Fc secures a long serum half-life and favourable pharmacokinetics due to its pH-dependent interaction with the neonatal Fc receptor (FcRn). FcRn also mediates transport of intact IgG across polarized epithelial barriers, a pathway that is attractive for delivery of Fc-containing therapeutics. So far, no study has thoroughly compared side-by-side how IgG and different Fc-fusion formats are transported across human polarizing epithelial cells. Here, we used an *in vitro* cellular transport assay based on the human polarizing epithelial cell line (T84) in which both IgG1 and Fc-fusions were transported in an FcRn-dependent manner. Furthermore, we found that the efficacy of transport was dependent on the format. We demonstrate that transepithelial delivery could be enhanced by Fc-engineering for improved FcRn binding as well as by Fc-polymerization. In both cases, transport was driven by pH-dependent binding kinetics and the pH at the luminal side. Hence, efficient transcellular delivery of IgG-based drugs across human epithelial cells requires optimal pH-dependent FcRn binding that can be manipulated by avidity and Fc-engineering, factors that should inspire the design of future therapeutics targeted for transmucosal delivery.

1. Introduction

Mucosal epithelial cells lining the gastrointestinal, respiratory and genital tracts [1–3] express the neonatal Fc receptor (FcRn) that interacts pH-dependently with the Fc part of immunoglobulin G (IgG) [4]. The receptor binds IgG at acidic pH (6.0), while no binding or release occurs at physiological pH (7.4) [5,6]. This mode of binding allows FcRn to transport IgG across epithelial barriers *via* the endosomal pathway [7,8]. While the polymeric Ig receptor (pIgR) mediates unidirectional basolateral to apical transport of IgA [9], several reports have demonstrated that FcRn mediates bidirectional transport of IgG across several epithelial cell types *in vitro* such as transfected rat kidney inner medullary collecting duct (IMCD) cells and Madine–Darby canine kidney (MDCK) cells, the human colon epithelial cell lines T84 and CaCo-2 as well as the placental trophoblast cell lines JAR and BeWo [10–17]. In addition, FcRn has been shown to mediate transport of IgG and IgG Fc fusions across different epithelial barriers *in vivo* [2,18–23] and *ex vivo* across a placental transfer model system [24,25]. As a result, mucosal secretions contain significant amounts of IgG [26,27], at levels that equal or exceed the levels of IgA in the lumen of the lower respiratory and female genital tracts [28,29]. In addition, human rectal secretions also contain high levels of IgG [30]. Interestingly, systemically administered IgG has been shown to protect against infections in the lung, intestine and female genital tract, and deficiencies in IgG increase the risk of both systemic and mucosal infections in humans and macaques [31–33].

The bidirectional mode of transport allows FcRn to translocate monomeric IgG into the lumen and retrieve them in the form of immune complexes (ICs). As such, studies in human FcRn (hFcRn) transgenic mice have demonstrated that the receptor participates in eradication of pathogens by directing IgG-bound antigens across the mucosal barrier for subsequent delivery to inductive mucosal sites [19,34]. Here exposure to dendritic cells (DCs) and presentation of antigenic peptides to T-cells results in protective immunity. Furthermore, FcRn is expressed by a subset of DCs in the lamina propria where it participates in cross-presentation of IgG ICs resulting in activation of cytotoxic T-cell responses [35,36]. Although it has been demonstrated that hFcRn transports monomeric IgG most efficiently in the basolateral to apical

* Corresponding author at: Centre for Immune Regulation (CIR), Department of Immunology, Oslo University Hospital, Rikshospitalet, University of Oslo, PO Box 4956, Oslo N-0424, Norway.
E-mail address: j.t.andersen@medisin.uio.no (J.T. Andersen).

http://dx.doi.org/10.1016/j.jconrel.2015.12.033
0168-3659/

direction [12], it is not clear whether formation of IgG ICs in the luminal environment increases transport from the apical to the basolateral side. Furthermore, the luminal environment of mucosal sites, such as the intestinal [37,38] and female genital [39,40] tracts are mildly acidic due to the activity of Na^+/H^+ exchangers [41]. This is thought to allow FcRn capture of IgG in the luminal space followed by receptor-mediated endocytosis. In contrast, uptake during physiological pH conditions is thought to occur solely *via* fluid phase pinocytosis, as recently clarified [42].

A number of studies have shown that FcRn expressed at mucosal surfaces may be used as a gateway for delivery of therapeutic proteins genetically fused to the Fc part of IgG. For instance, fusion of erythropoietin (EPO) to the Fc part of human IgG1 can be transported across the mucosal barrier in an FcRn-dependent manner upon pulmonary administration, resulting in greatly enhanced erythrocytosis [20,21]. Similarly, transepithelial delivery of Fc-fused subunit vaccines has been shown to require FcRn-dependent transport, which induced systemic and mucosal immunity that protected against infections [22,23]. Furthermore, Fc-coupled nanoparticles have been shown to be delivered across an airway-derived human epithelial cell line [43], and across gut epithelium *via* FcRn in mice [44]. Finally, pulmonary administered IgG has been shown to rely on FcRn for maintenance of post-absorption IgG levels in mice [45]. Although these studies demonstrate a great potential for the FcRn pathway in drug delivery, little focus has been given to how enhanced uptake and transport *via* FcRn may be achieved. Therefore, in this study, we established a protocol for an *in vitro* transcytosis assay based on the human epithelial cell line T84 [12] to compare FcRn-mediated transcellular transport of unlabelled IgG variants under non-inflammatory conditions. We present data showing that Fc-polymerization and the presence of an acidic luminal environment act synergistically with IgG Fc-engineering for improved FcRn binding [46–48] to enhance transcellular transport. Such knowledge is fundamental as it will guide the design of novel IgG-based drugs and vaccines tailored for optimal mucosal delivery.

2. Material and methods

2.1. Cell culture

All cell lines were acquired from ATCC. The T84 (human, colon carcinoma) cell line was maintained in DMEM/HAM's F12 (1:1), CaCo-2 (human, colorectal adenocarcinoma), CaLu-3 (human, lung adenocarcinoma), JURKAT (human, acute T-cell leukaemia), and U937 (human, histolytic lymphoma) were maintained in DMEM. Human embryonic kidney (HEK) 293E cells were maintained in RPMI (all from Life Technologies). Culture medium was supplied with 10% FCS, 2.5 mM L-glutamine, 25 μg/ml streptomycin and 25 U/ml penicillin (BioWhittaker), and the cells were incubated at 37 °C in a humidified 5% CO_2, 95% air incubator.

2.2. Commercial monoclonal Abs and Fc-fusions

The monoclonal Abs rituximab (human IgG1κ/Roche), infliximab (human IgG1κ/Janssen Biotechnology) and etanercept (human IgG1Fc-TNFRII/Pfizer) were purchased and storage buffer was exchanged with PBS containing 0.05% sodium azide (Sigma-Aldrich). The Fc part of rituximab was generated by papain digestion and purified using a HiTrap Protein G column (GE Healthcare). Protein size and purity was analysed by non-reducing SDS-PAGE. Construction and production of Fc hexamer variants have been described previously [49,50].

2.3. Recombinant IgG1 variants

A vector cassette system (pLNOH2-^{NIP}hIgG1-oriP) for sub-cloning of DNA sequences encoding Fc fragments into the framework of WT human IgG1 has been described [51]. The vector contains the heavy chain (HC) gene from human IgG1 with specificity for the hapten 5-iodo-4-hydroxy-3-nitro-phenacetyl (NIP), and was used for exchange of a panel of DNA fragments (synthesized by GenScript) encoding Fc-mutants, using the restriction sites AgeI and SfiI (C_H2 mutations) or SfiI and BamHI (C_H3-mutations); M252Y/S254T/T256E (MST), M428L/N434S (MN), H433K/N434F (HN) and M252Y/S254T/T256E/H433K/N434F (MST/HN). The Abs were produced by adherent HEK293E cells after transient co-transfection of the vectors together with a vector encoding a mouse λ light chain (LC) (pLNOH2-^{NIP}λLC-oriP) using Lipofectamine 2000 (Life Technologies) as previously described [52]. Construction of a plasmid encoding anti-NIP human IgG1 with the three Fc point mutations I253A/H310A/H435A (IHH) has been described [53], and the Ab was produced from a stably transfected J558L cell line. All Abs were purified from collected supernatants using a column coupled with a 4-hydroxy-3-nitrophenyl acetyl followed by size exclusion chromatography (SEC) using a Superdex 200 10/300 column (GE Healthcare) to obtain monomeric IgG1 variants. Fractions were up-concentrated using Amicon Ultra columns (Millipore).

2.4. Recombinant soluble human FcRn

Truncated monomeric His-tagged hFcRn was produced using a Baculovirus expression system, as described [24,54]. The viral stock were a kind gift from Dr. Sally Ward (University of Texas, Southwestern Medical Center, Dallas, USA). Secreted receptor was purified using a HisTrap HP column supplied with Ni^{2+} ions (GE Healthcare) that was pre-equilibrated with phosphate buffered saline (PBS) containing 0.05% sodium azide. The pH of the supernatant was adjusted with PBS/0.05% sodium azide (pH 10.9) to pH 7.2, and then applied to the column (5 ml/min) before washing using 200 ml of PBS followed by 50 ml of 25 mM imidazole/PBS (pH 7.2–7.4). Bound hFcRn was eluted with 50 ml of 250 mM imidazole/PBS (pH 7.2–7.4) following SEC using a HiLoad 26/600 Superdex 200 prep grade column (GE Healthcare) for isolation of monomeric receptor. Fractions eluted were concentrated using Amicon Ultra columns (Millipore) and stored at 4 °C. Construction of a eukaryotic vector with a cDNA encoding the three extracellular domains of soluble hFcRn lacking the transmembrane domain C-terminally fused to a gene encoding the *Schistosoma japonicum* gluthathione S-transferase (hFcRn-GST), as well as the gene for human β2-microglobulin (β2m) has been described [55,56].

2.5. RT-PCR and siRNA knockdown

Total cell RNA was isolated using the TRIzol reagent (Life Technologies) essentially as described by the manufacturer. cDNA synthesis was performed using 1 μg RNA and cDNA synthesis kit (Life Technologies). Isolated cDNA was amplified using the Phusion High Fidelity DNA polymerase (Finnzymes) together with gene specific primers. A siRNA mixture of three oligonucleotides specific for the human FcRn HC and control siRNA (Santa Cruz Biotechnology) was used according to the manufacturer instructions. RNA from siRNA treated cells was isolated at 0, 12, 48 and 72 h post transfection, followed by RNA isolation, cDNA synthesis and RT-PCR as described above. RT-PCR products were analysed by gel electrophoresis.

2.6. Cellular staining

T84 cells were seeded on glass slides (Thermo Fisher Scientific) and grown to 90% confluence. Cells were then fixed in acetone for 10 min and air-dried, before washing in PBS and staining using ADM31, an anti-hFcRn specific mouse IgG2b antibody [57]. ADM31 was diluted in PBS with 1.25% bovine serum albumin (BSA) to a final concentration of 5 μg/ml, and incubated with T84 cells for 90 min. Mouse IgG2b with irrelevant specificity (R&D Systems) was used as isotype control. The cells were washed for 2 min in PBS, followed by incubation with an Alexa-488 conjugated anti-mouse IgG antibody (Life Technologies).

Subsequently, cells were washed in PBS, incubated with Hoechst solution for 2 min and washed in dH_2O, followed by mounting on cover glass using polyvinyl alcohol (Sigma-Aldrich) and left to dry O/N at 4 °C. Confocal images were acquired using an Olympus FluoView1000 microscope equipped with a PlanApo 60/1.35 oil objective (Olympus). Image acquisition was done by sequential line scanning. Images were processed using Image J (National Institute of Health) and Adobe Illustrator (Adobe Systems Inc).

2.7. Differential scanning fluorimetry (DSF)

Protein stability of monoclonal Abs and Fc-fusions were measured by DSF using a Lightcycler RT-PCR instrument (Roche). SYPO Orange (Sigma-Aldrich) was mixed (1:1000 dilution) with the Abs (0.1 mg/ml) in 25 μl PBS. Samples were run in triplicates in 96 well Lightcycler 480 multiwell plates. The RT-PCR instrument was programmed to ramp the temperature from 25 °C to 95 °C after a period of 10 min at 25 °C. Data were collected every 0.5 °C using the 450 nm excitation and 568 nm emission filters. Data transformation and analysis was performed using the DSF analysis protocol essentially as described [58].

2.8. Transcytosis assay

Transwell filters (1.12 cm^2) with collagen coated polytetrafluoroethylene (PTFE) membranes and 0.4 μm pore size (Corning Costar) were incubated overnight in complete growth medium followed by seeding of 1.0×10^6 T84 cells per well. Cells with a passage number from 1 to 4 were used for all experiments due to easier growth and improved polarization properties compared to higher passage numbers. Transepithelial electrical resistance (TEER) was monitored daily using a MILLICELL-ERS-2 V-ohm meter (MILLIPORE). The cultures were grown for 4–5 days before reaching confluence with a TEER value of ~1000–1300 $\Omega \cdot cm^2$. Prior to experiments the monolayers were starved for 1 h in Hank's Balanced Salt Solution (HBSS). For transport experiments at acidic pH, HBSS was buffered to pH 6.0 by addition of MES buffer (Sigma-Aldrich). This was controlled by collecting a minor volume of the medium for testing on a Hydrion short range pH paper (Micro Essential Laboratories). Then, 200 nM of either NIP-specific IgG1 variants, infliximab, rituximab or etanercept were added to either the apical or the basolateral transwell chamber. Fc hexamers (polyFc-L309C or polyFc-L309C/H310L) [49] were added at an Fc ratio of 200 nM. Immune-complexes (ICs) containing anti-NIP IgG1 variants and NIP-conjugated ovalbumin (OVA) (Biosearch Technologies) was formed by incubating 200 nM NIP-specific IgG1 variants with 50 nM NIP-OVA in 10 μl PBS for 1 h at RT prior to transcytosis experiments. Samples were collected from the opposite reservoir at 0, 1, 2 and 4 h for initial experiments and after 0 and 4 h for remaining experiments. Where stated, T84 monolayers were treated with 0.1 μM Bafilomycin A1 (Sigma-Aldrich) added 20 min prior to and during experiments.

2.9. Quantification of IgG transport by ELISA

96-well Maxisorp plates (NUNC) were coated with either NIP-conjugated BSA (Biosearch Technologies) or a goat polyclonal anti-human Fc specific antibody (locally produced) diluted to 1 μg/ml in PBS. The plates were blocked with 4% skimmed milk in PBS (Acumedia) (S/PBS) for 2 h at RT, followed by washing 4 times with PBS/Tween20 (T). Samples collected during transcytosis experiments were diluted 1:1 in S/PBS/T, added to wells and incubated for 1 h at RT before washing as above. Captured anti-NIP IgG1 variants were detected using a horseradish peroxidase (HRP)-conjugated anti-mouse λ LC antibody (Southern Biotech), while captured rituximab, infliximab, etanercept, NIP-IgG IC and Fc hexamers were detected with a polyclonal alkaline phosphatase (ALP)-conjugated anti-human Fc antibody produced in goat (Sigma-Aldrich). Binding was visualized by addition of either 100 μl 3,3′,5,5′-tetramethylbenzidine substrate (TMB) (CalBiochem) or ALP substrate (Sigma-Aldrich). The TMB-HRP reaction was terminated by addition of 100 μl 1 M HCl. Absorbance was recorded at 450 nm (HRP) or 405 nm (ALP) using a TECAN Sunrise spectrophotometer. The picomolar amount per surface area (pM/cm^2) of transported protein was determined from standard curves of each individual Ab, Fc-fusion, IC or polyFc-fusion.

2.10. Surface Plasmon resonance (SPR)

Determination of binding kinetics was performed using a BIAcore 3000 instrument (GE Healthcare). Abs and Fc-fusions were immobilized on CM5 chips at ~550 resonance units (RU), using the amine coupling kit provided by the manufacturer. Unreacted moieties on the CM5 surface were blocked with 1 M ethanolamine. For all experiments, phosphate buffer (67 mM phosphate, 0.15 M NaCl, 0.005% Tween20) at pH 6.0, or HBS-P buffer (0.1 M HEPES, 0.15 NaCl, 0.005% surfactant P20) at pH 7.4 were used as running and regeneration buffers, respectively. Kinetics measurements were performed using serial dilutions of monomeric hFcRn injected using the pH 6.0 buffer at a flow rate of 40 μl/min at 25 °C. In addition, hFcRn was immobilized (~550 RU) and equal amounts of the Fc hexamers were injected as above. To correct for non-specific binding and bulk buffer effects, responses obtained from a control CM5 surface and blank injections were subtracted from each interaction curve. Kinetic rate values were calculated using either a simple Langmuir 1:1 ligand binding model or a steady state affinity model provided by the BIA evaluation 4.1 software.

3. Results

3.1. Characterization of the cell line T84

To compare how human IgG1 Abs and Fc-fusions formats are transported by FcRn across polarized layers of human epithelial cells, we established a protocol for a transwell system where a human mucosa derived epithelial cell line could be cultured to monolayers within a few days. First, we used RT-PCR to detect mRNA transcripts of hFcRn HC and β2-microglobulin (β2m), in three human epithelial cell lines, namely T84, CaCo-2 and CaLu-3. The cell lines JURKAT (human T-cell line) and U937 (human monocyte cell line) were included as negative and positive controls for hFcRn expression respectively [59]. T84 cells were shown to express both hFcRn HC and β2m, and the levels of amplified mRNA transcripts were comparable to that found in CaCo-2, CaLu-3 and U937, while no amplification of the HC was detected in JURKAT cells (Fig. 1A). Furthermore, the monocyte cell line, but none of the epithelial cell lines or JURKAT cells were shown to express the classical IgG binding receptor FcγRIIb (Fig. 1A), the only classical FcγR expressed by non-haematopoietic cells [60].

Invariant chain (Ii) is up-regulated in non-professional cells during inflammation [61]. Furthermore, Ii has been shown to interact with FcRn, however, the impact of this association is not fully understood [62]. Transcripts of the human Ii splice variants (p33/p35) and (p41/p43) [63] were amplified from CaCo-2 and CaLu-3 as well as U937, while no transcripts were observed in JURKAT and T84 (Fig. 1B). Thus, while CaCo-2 and CaLu-3 expressed Ii, T84 did not, and thus the latter have the characteristics of a non-inflammatory state, as previously observed [61]. Therefore, we used T84 for further experiments and verified the expression of hFcRn at the protein level by staining cells using ADM31, a mouse monoclonal anti-hFcRn Ab specific for the HC [57,64] (Fig. 1C). In addition, endogenous expression of hFcRn HC mRNA transcripts was verified using a mixture of three siRNAs, which knocked down the expression completely 48 h post transfection (Fig. S1).

Finally, we tested growth of T84 cells in a transwell system, by seeding cells on collagen coated filter inserts. The formation of polarized monolayers was followed by measurement of transepithelial electrical resistance (TEER). The cells reached high TEER values 4–5 days post seeding (1000–1300 $\Omega \cdot cm^2$) (Fig. 1D), while CaCo-2 and CaLu-3 took

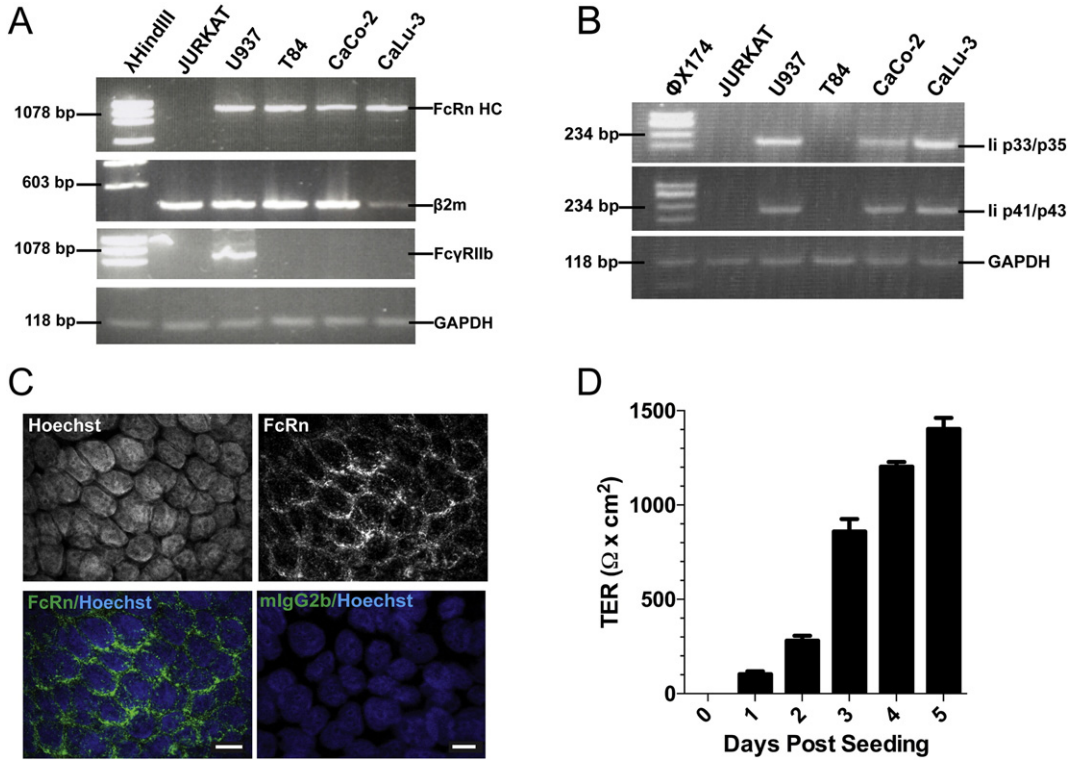

Fig. 1. Characterization of the human epithelial cell line T84. (A) RT-PCR showing amplification of hFcRn HC, β2m and FcγRIIb mRNA transcripts isolated from the human epithelial cell lines T84, CaCo-2 and CaLu-3. JURKAT (T-cell line) and U937 (monocytic cell line) were included as negative and positive controls, respectively. Amplification of GAPDH mRNA transcripts was used as a housekeeping control. (B) RT-PCR showing amplification of Ii splice variants (p33/p35) and (p41/p43) mRNA transcripts from the human epithelial cell lines T84, CaCo-2 and CaLu-3. Controls as in (A). (C) Staining of T84 cells using the anti-hFcRn HC antibody ADM31. A mouse IgG2b antibody was used as an isotype control. FcRn is shown in green while Hoechst staining was included to visualize the nucleus (blue). Scale bars are 10 μm. (D) Transepithelial electrical resistance (TEER) ($\Omega \cdot cm^2$) measured over four developing monolayers of T84 cells from 0 to 5 days post seeding. Error bars indicate S.D.

up to 3 weeks to form polarized monolayers (data not shown). Importantly, the protocol established rely on seeding of T84 cells with a passage number of 1–4 as cells with higher passage numbers were found to form polarized monolayers less well within 5 days (data not shown). Hence, these results show that the T84 cell line expresses hFcRn endogenously, but neither FcγRIIb nor Ii and forms polarized monolayers with high TEER, which makes it an ideal human epithelial model cell line for investigation of FcRn-mediated transport under non-inflammatory conditions.

3.2. FcRn-mediated IgG transport in T84 cells

We demonstrated specific FcRn-mediated transcellular transport of IgG across polarized T84 cells grown on transwell filters using monoclonal human IgG1 Abs with specificity for the hapten NIP. One contained the WT sequence, and one had three Fc amino acid substitutions at the core of the FcRn interaction site, where residues I253, H310 and H435 were mutated to alanine (IgG1-IHH) (Fig. 2A), which abrogate FcRn binding [52]. Transcytosis experiments were performed by adding

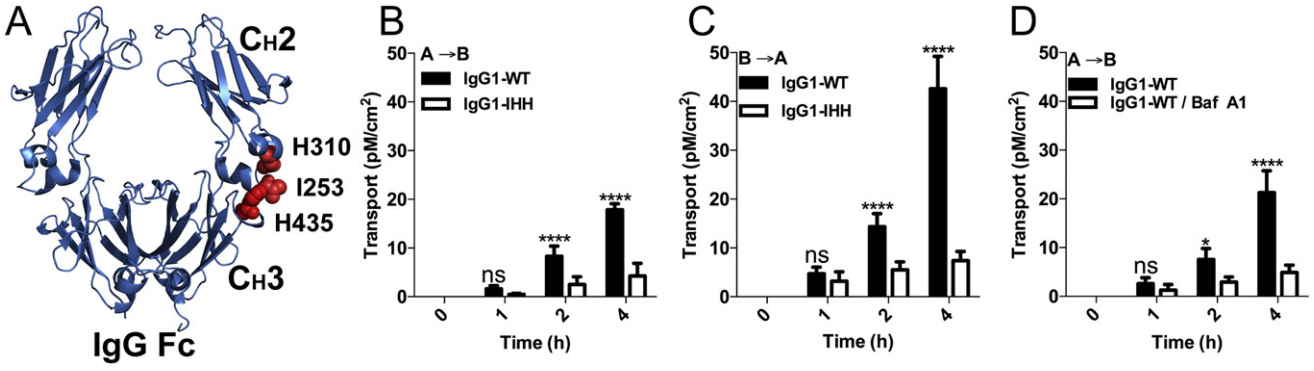

Fig. 2. FcRn mediated bidirectional flux of IgG across polarized T84 monolayers. (A) A structural illustration showing the Fc part of human IgG1 (blue). The three key FcRn interacting residues I253, H310 and H435 are shown as red spheres. The figure was prepared using PyMOL (DeLano Scientific) and based on the PDB structure 1HZH [99]. (B) Transwell assay showing apical to basolateral transport of NIP-specific IgG1-WT and IgG1-IHH across polarized T84 monolayers at 0, 1, 2 and 4 h post adding. Presented as pM/cm^2. (C) Basolateral to apical transport of NIP-specific IgG1-WT and IgG1-IHH across polarized T84 monolayers at 0, 1, 2 and 4 h post adding. Presented as in (B). (D) Apical to basolateral transport of NIP-specific IgG1-WT across polarized T84 monolayers in the absence and presence of 0.1 μM Bafilomycin A1. Presented as in (B). Error bars indicate S.D. of four individual monolayers from one representative experiment out of three. *$p < 0.05$, **$p < 0.001$, ***$p < 0.0005$, ****$p < 0.0001$; ns: not significant, by two-way ANOVA test (Sidak's).

the two IgG1 variants to either the apical or basolateral reservoir of the transwell system, and samples were collected from the opposite side of the monolayer after 0, 1, 2, and 4 h. Both the apical and the basolateral chambers were buffered to physiological pH. The amounts of transported IgG1 variants were determined after capture on NIP-conjugated BSA using ELISA, and subsequently fitted to a standard curve for quantification. IgG1-WT was transported 3–4 fold more efficiently than IgG1-IHH, both in the apical to basolateral and the basolateral to apical direction (Fig. 2B-C). In addition, basolateral to apical transport was 2.0–2.5-fold more efficient than apical to basolateral transport, which is in line with previous observations [12,65]. Next, transport of IgG1-WT was addressed in the presence of Bafilomycin A1, an inhibitor of the H^+ ATPase, which causes the endosomal pH-gradient to collapse [66]. The results showed reduced transport of IgG1-WT from the apical to the basolateral side in the presence of Bafilomycin A1 (Fig. 2D). Thus, bidirectional transport of IgG1 across polarized T84 cells was shown to be strictly dependent on FcRn engagement and an acidic endosomal environment.

3.3. Transport of IgG Abs and Fc-fusion across polarized T84 cells

Next, the transport of two IgG1-based therapeutics used in the clinic, namely infliximab and rituximab as well as one Fc-fusion, etanercept (TNFRII fusion) [67] were measured. As several reports have shown that the Fab may influence FcRn binding and half-life of therapeutic IgG1 molecules [68–71], we also included an Fc-fragment of rituximab. Monomeric fractions of all proteins were isolated by SEC followed by non-reducing SDS-PAGE and Coomassie staining, which showed migration of pure monomeric fractions with expected molecular weights (Fig. 3A). To determine their hFcRn binding properties, we measured the binding affinity using SPR by injecting titrated amounts of the monomeric receptor over immobilized infliximab, rituximab and etanercept at pH 6.0. Fitting the obtained sensorgrams to a steady state affinity model revealed that infliximab, rituximab and etanercept bound with KD values of 0.78 μM (Fig. 3B-C), 1.0 μM (Fig. 3D-E) and 0.94 μM (Fig. 3F-G), respectively. As expected, no hFcRn binding were detected at pH 7.4 (Fig. S2). Using differential scanning fluorimetry (DSF), we also found that they all had a melting temperature of 70 °C (Fig. S3). We then used polarized T84 cells in the transwell system and measured apical to basolateral transport 4 h post addition of equal molar amounts of infliximab, rituximab, rituximab Fc and etanercept. The amount of transport were determined by an anti-Fc ELISA. The results showed that all molecules were transported equally well (Fig. 3H). Thus, the removal of the Fab arms as well as genetic fusion of TNFRII to the Fc part of IgG1, do not affect FcRn binding or transcellular delivery.

3.4. Fc-engineering enhances transcytosis

FcRn does not only direct transcytosis of IgG, as the receptor is also expressed by endothelial cells and DCs where it salvages IgG from systemic degradation [53,72], and therefore, the half-life of IgG is 3 weeks in humans compared to only a few days for other Ab isotypes [73]. Fc-engineering of Abs that increases binding to FcRn at acidic pH while retaining weak binding at physiological pH has been shown to result in IgG variants with prolonged *in vivo* serum half-life [74–76], and recently, the maximum affinity threshold at physiological pH that still results in FcRn-mediated rescue of IgG has been determined [77]. Furthermore, evidence obtained using an *ex vivo* placental transfer model supports that such engineering enhances FcRn-mediated transport across cellular barriers [76]. However, a side-by-side comparison of Fc-engineered human IgG1 variants has yet to be reported in a transcytosis assay. Therefore, we generated four Fc-engineered IgG1 variants with NIP specificity that have previously been reported to alter FcRn pH-dependent binding and pharmacokinetics (Fig. 4A). One Ab harbours three mutations in the C_H2-domain, IgG1-M252Y/S254T/

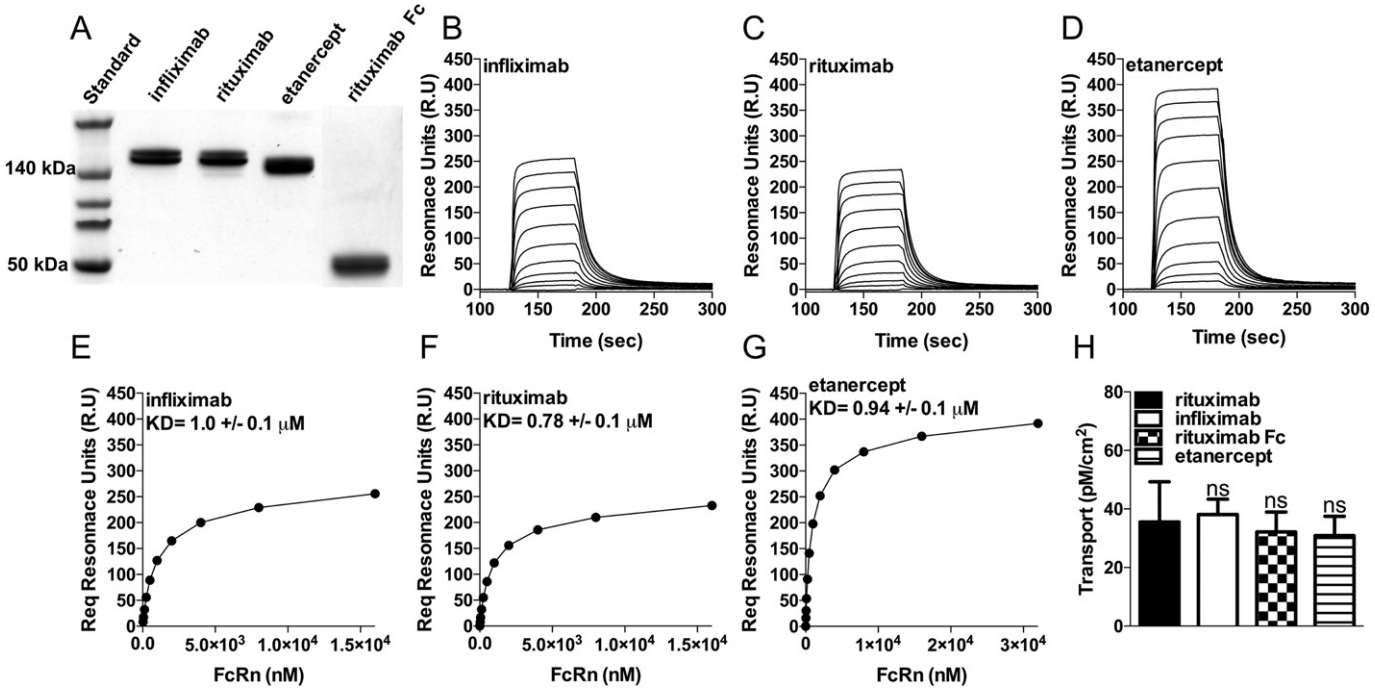

Fig. 3. Differential FcRn mediated delivery of commercial IgG-based drugs. (A) Non-reducing SDS-PAGE showing migration of monomeric fractions of rituximab (150 kDa), infliximab (150 kDa), etancercept (150 kDa), and rituximab Fc (50 kDa). The 140 kDa and 50 kDa band of the protein standard (260–10 kDa) is indicated. (B–D) Representative SPR sensorgrams showing binding of titrated amounts of monomeric hFcRn injected over immobilized commercial mAbs and Fc-fusion (~550 R.U.) at pH 6.0. The injections were performed at 25 °C and the flow rate was 40 μl/min. (E–G) Steady state affinity constants were determined by plotting equilibrium binding responses (Req) *versus* injected concentrations of monomeric hFcRn using the BIAevaluation 4.1 software. (H) Transwell assay showing apical to basolateral transport of rituximab, infliximab, rituximab Fc and etanercept across polarized T84 monolayers 4 h post adding. Presented as pM/cm^2. Error bars indicate S.D. of four individual monolayers from one representative experiment out of three. ns: not significant, by one-way ANOVA test (Dunnetts).

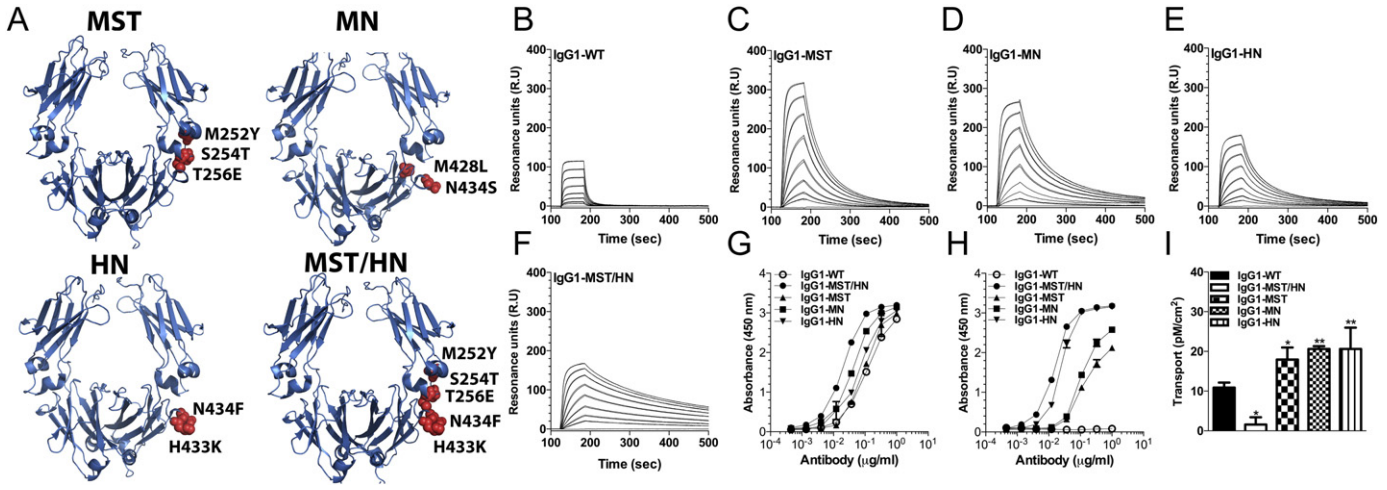

Fig. 4. FcRn binding and transport of IgG1 Fc-engineered variants. (A) Structural illustration showing the Fc part (blue) of human IgG1. Amino acid substitutions included in different variants engineered for improved hFcRn binding are shown as red spheres. The figure was prepared using PyMOL and was based on the Protein Data Bank structure 1HZH [99]. (B–F) Representative SPR sensorgrams showing binding of titrated amounts of monomeric hFcRn (31.25–4000.0 nM) injected over immobilized Fc-engineered NIP specific IgG1 variants (~550 R.U.) at pH 6.0. The injections were performed at 25 °C and the flow rate was 40 μl/min. (G) ELISA showing binding of Fc-engineered NIP specific IgG1 variants towards hFcRn-GST at pH 6.0 and (H) pH 7.4. Error bars indicate S.D. of duplicates from one representative experiment out of three. (I) Transwell assay showing apical to basolateral transport of NIP-specific Fc-engineered IgG1 variants across polarized T84 monolayers 4 h post addition. Presented as pM/cm^2. Error bars indicate S.D. of four individual monolayers from one representative experiment out of three. *$p < 0.05$, **$p < 0.001$, ***$p < 0.0005$, ****$p < 0.0001$, ns: not significant, by one-way ANOVA test (Dunnetts).

T256E (IgG1-MST) [74,78], while two Abs harbour two amino acid substitutions in the C_H3 domain, IgG1-H433K/N434F (IgG1-HN) [76] and IgG1-M428L/N434S (IgG1-MN) [75]. The MST variant showed 10-fold improved binding to FcRn at acidic pH with retained pH-dependence that resulted in 3.7 and 3.5-fold extended half-life in cynomolgus monkeys and humans, respectively [74,78]. While the MN variant showed 11-fold improved binding and 3.2-fold extended half-life in cynomolgus monkeys [75]. The last Ab contains five Fc-mutations, IgG1-M252Y/S254T/T256E/H433K/N434F (IgG1-MST/HN) [79–81], which disrupts pH-dependence by improving binding both at acidic and neutral pH. The latter, so-called Abdeg (Ab for degradation) molecule consequently has a very short serum half-life [79].

Next, we determined the binding kinetics of the Fc-engineered Abs towards hFcRn at pH 6.0 using SPR. Compared to WT, IgG1-MST, IgG1-HN and IgG1-MN showed 13, 19, and 21-fold improved KD-values, respectively, while IgG1-MST/HN bound the receptor with 100-fold better affinity than the WT (Fig. 4B-F; Table 1). In addition, we used ELISA to measure binding of the Fc-engineered Abs to hFcRn at both pH 6.0 and 7.4. The results showed a similar trend of binding at pH 6.0 as that measured by SPR (Fig. 4G), while the following hierarchy of binding was observed at pH 7.4; MST/HN > HN > MN > MST > WT (Fig. 4H).

Finally, to address the impact of Fc-engineering on transport across polarized human epithelial cells, equal molar amounts (200 nM) of the Abs were added to the apical reservoir of the transwell system in parallel with the parental WT, and the amounts transported after 4 h were quantified by ELISA. The data reveal that the MST, HN and MN variants were transported 1.6, 1.8 and 1.9-fold more efficiently than IgG1-WT while the Abdeg variant was not detected in the basolateral chamber, due to poor transport or release (Fig. 4I). Hence, improved pH-dependent binding to FcRn at acidic pH results in enhanced FcRn-mediated delivery across human polarized epithelial layers.

Table 1
| SPR-derived kinetics for binding of human IgG1 variants to human FcRn.

hIgG1 variants	Ka (10^4/Ms)	Kd (10^{-2}/s)	KD (nM)[a,b]
hFcRn			
WT	8.5 ± 0.5	9.5 ± 0.4	1117.6
MST	19.4 ± 0.4	1.7 ± 0.0	87.6
HN	20.1 ± 0.1	1.2 ± 0.1	59.7
MN	17.5 ± 0.6	0.9 ± 0.0	51.4
MST/HN	27.4 ± 0.4	0.3 ± 0.1	10.9

[a] The kinetic rate constants were obtained using a simple first-order (1:1) Langmuir bimolecular interaction model. The kinetic values represent the average of triplicates.
[b] The steady-state affinity constants were obtained using an equilibrium (Req) binding model supplied by the BIAevaluation 4.1 software. The affinities derived from equilibrium binding data represent the average of triplicates.

3.5. IgG-containing ICs are transported more efficiently than monomeric IgG

IgG-containing ICs can be transcytosed by FcRn from the apical to the basolateral side where they are captured by DCs in the lamina propria resulting in activation and induction of immunity [19,34]. Given the fact that apical to basolateral transport of monomeric IgG is less efficient than in the opposite direction (Fig. 2) [12], we hypothesised that IC formation in the lumen may be a general mechanism to achieve more efficient transport to the basolateral side. Therefore, we investigated how IgG containing ICs were transported relative to monomeric IgG in the T84 transwell system. We used NIP-specific IgG1-WT and IgG1-MN (200 nM) that were mixed 4:1 with NIP-conjugated OVA to form ICs. The ICs were then added to the apical side of polarized T84 cells, and transport was compared to that of their monomeric counterparts (200 nM). Quantification using ELISA based on anti-Fc standard curves, showed that IgG1-WT:NIP-OVA ICs were transported 2-fold more efficiently than the monomeric WT Ab, while IgG1-MN:NIP-OVA ICs were transported 2-fold more efficiently than the monomeric MN Ab (Fig. 5A). Compared with monomeric IgG1-WT, 3-fold more of ICs containing IgG1-MN were delivered across the cellular layers. Taken together, the data demonstrate that IgG-containing ICs are more efficiently shuttled by FcRn in the apical to basolateral direction than monomeric WT-IgG1, and that the avidity effect obtained by IC formation can act synergistically with Fc-engineering to enhance delivery.

3.6. Acidic apical pH enhances FcRn-mediated delivery

Previous reports have suggested that a mildly acidic environment at the apical luminal side of mucosal surfaces allows more efficient uptake due to IgG binding to surface displayed FcRn [72,79,82]. To address this, we compared the transport efficiency of monomeric IgG1-WT with that of IgG1-MN when the apical reservoirs of the transwell system were buffered to either pH 6.0 or 7.4. The pH of the basolateral chamber

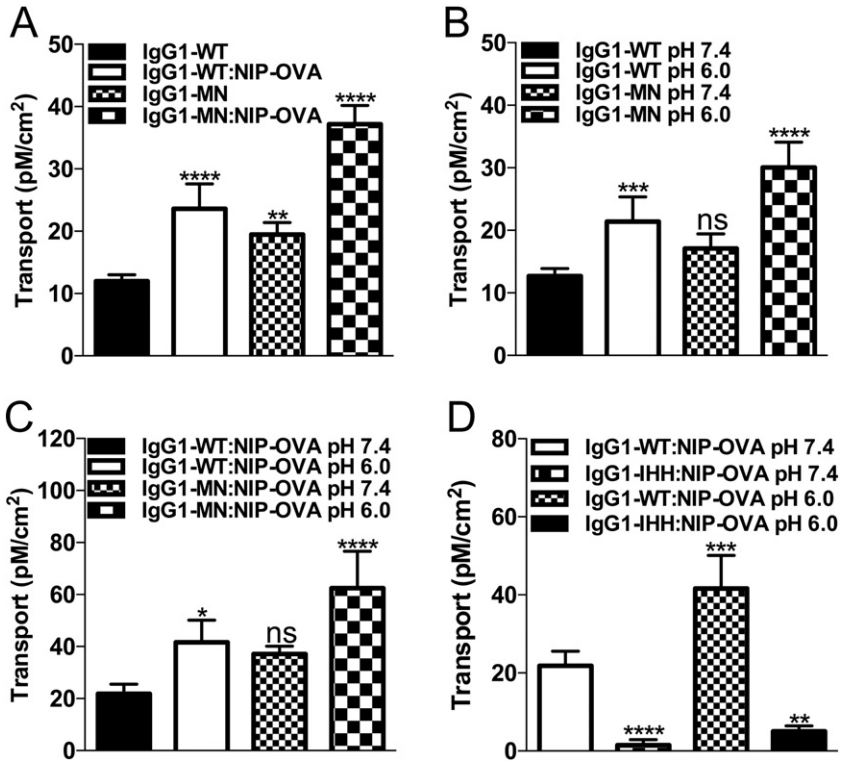

Fig. 5. Synergistic enhancement of FcRn-mediated transcellular transport. (A) Apical to basolateral transport of monomeric IgG1-WT, monomeric IgG1-MN, IgG1-WT:NIP-OVA and IgG1-MN:NIP-OVA ICs across polarized T84 monolayers 4 h post addition. Presented as pM/cm^2. (B) Apical to basolateral transport of monomeric IgG1-WT or IgG1-MN across polarized T84 monolayers at either an acidic (6.0) or physiological (7.4) apical pH environment. Presented as in (A). (C) Apical to basolateral transport of IgG1-WT:NIP-OVA and IgG1-MN:NIP-OVA complexes across polarized T84 monolayers at either acidic (6.0) or physiological (7.4) apical pH environment. Presented as in (A). (D) Apical to basolateral transport of IgG1-WT:NIP-OVA and IgG1-IHH:NIP-OVA complexes across polarized T84 monolayers at either an acidic (6.0) or physiological (7.4) apical pH environment. Presented as in (A). Error bars indicate S.D. of four individual monolayers from one representative experiment out of three. *$p < 0.05$, **$p < 0.001$, ***$p < 0.0005$, ****$p < 0.0001$, ns: not significant, by one-way ANOVA test (Dunnetts).

was kept constant at pH 7.4 during all experiments. Notably, exposure of the basolateral side of the polarized cell layers to acidic buffer (pH 6.0) compromised the integrity of the monolayers and transcellular resistance was as a consequence lost (data not shown). The results showed an increase of 1.7-fold with the apical reservoir kept at pH 6.0 relative to physiological pH (Fig. 5B). The synergistic effect of acidic pH and Fc-engineering translated into a 2.8-fold increase in transcellular delivery of IgG1-MN. Importantly, the pH of the basolateral reservoir did not change during the 4 h of incubation, which illustrates how well the T84 cell line forms monolayers of polarized cells (data not shown).

Given the fact that avidity increased the rate of transport across polarized T84 monolayers, we compared how luminal pH affects transport of the ICs IgG1-WT:NIP-OVA and IgG1-MN:NIP-OVA. Here, a similar effect of pH was measured for both ICs, as ~2-fold more of each IC were delivered across the cell layers when the apical side was acidified (Fig. 5C). When apical to basolateral transport of monomeric IgG1-WT at neutral apical pH was compared with that of IgG1-MN:NIP-OVA at pH 6.0, the increase in delivery was 5.2-fold. The FcRn dependence was demonstrated by the fact that no IgG1-IHH:NIP-OVA was detected in the basolateral reservoir at either pH condition (Fig. 5D). Thus, our findings support that an acidic apical environment leads to more efficient uptake, transport and release to the opposite side of the polarized cell layer.

3.7. Polymerization of Fc-fusions may allow for more efficient delivery across polarized cells in an FcRn-dependent manner

The success of Fc-fusions as therapeutics has led to development of new formats with improved properties tailored for particular applications [83,84]. One such format is hexamers of IgG1 Fc fragments formed by adding the 18 amino acid tailpiece of human IgM to the C-terminal end of the HC in combination with the C_H2 mutations L309C and H310L [50]. Since H310 of the C_H2-domain is a key residue in pH-dependent FcRn binding [85,86], we recently tested similar molecules without the H310L mutation, and found it to be dispensable as polyFc-L309C (Fig. 6A) was readily formed and also bound hFcRn by ELISA [49] and SPR (Fig. S4). As IgG IC formation improves FcRn-dependent transcellular delivery, we compared apical to basolateral transport of a full-length IgG (infliximab) with that of the two polyFc variants polyFc-L309C and polyFcL309C/H310L at equal molar Fc concentration (200 nM), again using polarized T84 monolayers. Following 4 h of incubation, the amounts transported were quantified by ELISA, which revealed that polyFc-L309C was transported 9-fold more efficiently than monomeric infliximab when given at acidic pH, while polyFc-L309C/H310L was not transported (Fig. 6B). A similar trend was measured when given at pH 7.4, as polyFc-L309C was transported 6.5-fold more efficiently than infliximab (Fig. 6C). Comparing transport at the two different pH conditions, we found that 3-fold more of polyFc-L309C was delivered when added to an apical reservoir buffered to pH 6.0 than when provided at physiological pH. Thus, our results show that polymerization of Fc-fusion scaffolds has a great effect on its capacity to be delivered efficiently in an FcRn-dependent manner across polarized human epithelial cells.

4. Discussion

In this study we demonstrate that FcRn-mediated transmucosal delivery can be enhanced synergistically by Fc-engineering, IgG IC formation and the presence of an acidic luminal environment. In addition, we found that Fc hexamers is more efficiently transcytosed by FcRn compared to monomeric IgG. Although a major goal of the biopharmaceutical industry has been to prolong the serum half-life of IgG-based drugs

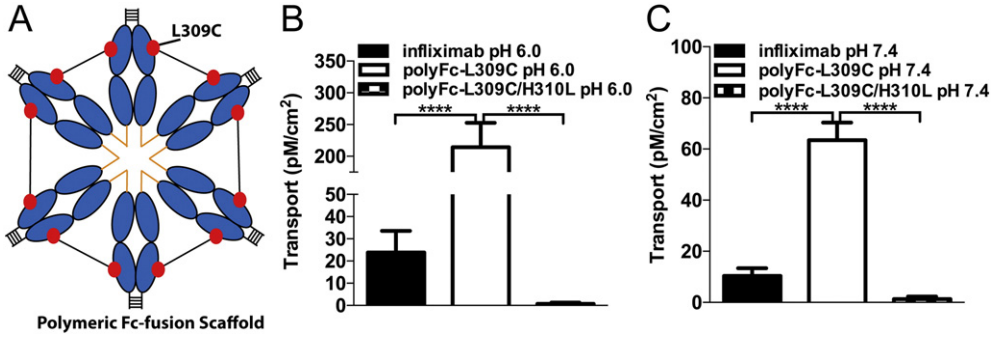

Fig. 6. Enhanced FcRn-mediated transcellular delivery of a polymeric Fc-fusion format. Apical to basolateral transport of infliximab, polyFc-L309C and polyFc-L309C/H310L across polarized T84 monolayers at either an (A) acidic (6.0) or (B) physiological (7.4) apical pH environment. Presented as pM/cm^2. Error bars indicate S.D. of four individual monolayers from one representative experiment out of three. *p < 0.05, **p < 0.001, ***p < 0.0005, ****p < 0.0001, ns: not significant, by one-way ANOVA test (Tukey's).

by engineering binding to FcRn [46–48], the potential benefits of mucosal transcellular delivery warrants a thorough investigation of how drugs can be designed in order to achieve optimal transport efficacy. Such knowledge is of fundamental importance for both design and site of administration of IgG-based fusion therapeutics.

We established a protocol for an *in vitro* transcytosis assay based on the human epithelial cell line T84, which express FcRn endogenously and transports IgG in an FcRn dependent manner, consistent with previous reports [12,61]. We found that an Fc fragment derived from rituximab was transported equally across polarized epithelial cells as the full-length antibody and the TNFRII Fc-fusion etanercept. This was in line with kinetic measurements showing that the fusion bound equally well as full-length therapeutic antibodies to FcRn. Thus, the Fab arms of rituximab are not required for efficient transport and genetic fusion of TNFRII to the Fc fragment does not interfere with binding to FcRn and transepithelial transport.

Given the importance of the FcRn pathway as a delivery route, it is crucial to determine features of IgG and Fc-fusions that either compromise or enhance transport to secure optimal transcellular delivery. Here, we found that IgG1 molecules containing site-specific amino acid substitutions in the Fc part, which enhance pH-dependent FcRn binding by 13 to 21-fold at acidic pH, were transported 1.6 to 1.9-fold more efficiently than the WT counterpart. Thus, IgG1 Fc-engineering, which leads to prolonged serum half-life is also improving delivery *via* FcRn across polarized epithelial cells. The increase in transcellular transport of the mutant variants measured after 4 h in the transwell system was not directly comparable with the reported half-life values for the same variants. For instance, IgG1-MST gained 3.7 and 3.5-fold prolonged serum persistence in cynomolgus monkeys and humans, respectively [74,78], while IgG1-MN gained 3.2-fold longer half-life in cynolomolgus monkeys [75], and IgG1-HN has demonstrated 2-fold improved transport in an *ex vivo* placental transfer model system [76]. Interestingly, the extended half-life of the MN variant has been shown to improve anti-tumour activity in a xenograft mouse model [75], and in another example, introduction of the mutations into an IgG1 with anti-simian immunodeficiency virus (SIV) specificity resulted in enhanced protection against SIV challenge in non-human primates due to increased FcRn dependent mucosal localization of the Ab [87]. In addition, the MN mutations have been incorporated into an IgG1 Fc fusion containing the cytotoxic T-lymphocyte-associated protein 4 (CTLA4; abatacept), which improved binding to hFcRn by 7.6-fold and resulted in 1.4-fold extended serum half-life in cynomolgous monkeys [88]. Notably, CTLA-4 was also engineered for improved binding towards CD80/CD86, which likely explains the shorter half-life compared with IgG1-MN, as recently reviewed [89]. Thus, improvements in FcRn binding kinetics do not directly correlate with the same fold of extended half-life or transcellular transport. The reasons for this may be related to the experimental setup and the complexity of intracellular trafficking of the Ab variants through the intracellular pH-gradient of different cell types. When it comes to polarized epithelial cells, IgG that has been transported *via* FcRn may potentially re-enter the cells and either be transported across the cells or be recycled back to the basolateral side for release again [17]. Thus, several pathways may operate simultaneously, and the amounts of IgG variants accumulating at the opposite side of the cell layer at a given time are therefore a result of the sum of these processes. That said, IgG has to first enter the cells and then be delivered across the cells *via* a transcytotic pathway for release at the opposite side of the cells.

Our finding that IgG-containing ICs are transported more efficiently across human polarized epithelial cells in the apical to basolateral direction compared to monomeric IgG may be a mechanism of immunological importance that has evolved to secure efficient delivery of IgG-ICs to DCs at mucosal inductive sites. In stark contrast, studies using endothelial cells and DCs have demonstrated that IgG containing ICs are routed away from recycling endosomes and into the lysosomal pathway in an FcRn dependent manner [35,53,90]. The mechanism responsible for the differences observed in FcRn-dependent handling of IgG-ICs in different types of cells are not entirely clear and need further investigation. One possibility is that enhanced transcellular transport of IgG-ICs could be a result of FcRn cross-linking in the transcytotic vesicles. However, we cannot rule out that the size of the ICs may influence trafficking, and that a higher degree of cross-linked FcRn molecules may result in delivery to the lysosomal pathway in polarized epithelial cells, as previously indicated [90]. Interestingly, it was recently demonstrated that IgG in complex with monomeric ligands bound FcRn with decreased affinity, while IgG in complex with multimeric ligands compensated for decreased binding by avidity [91].

Furthermore, we show that a hexameric Fc fusion format leads to enhanced FcRn-mediated delivery across polarized cells. Thus, coupling of therapeutic proteins or vaccine subunits to this scaffold could be an attractive approach to ensure optimal mucosal delivery. However, whether or not genetic fusion will affect FcRn binding and transport properties will probably depend on the nature of the fused molecules, a topic that should be addressed in each case. Steric hindrance may be one challenge, as previously shown for an IgG1 Fc fusion where EPO was genetically fused to one of the HCs that resulted in more efficient delivery across epithelial lung barriers in both primates and humans compared to a fusion harbouring two EPO molecules [20,21]. As such, the number of fused therapeutic molecules, as well as the degree of Fc polymerization should be considered when designing this type of drugs. Moreover, the mucosal route of delivery may be particularly relevant for multivalent Fc based mucosal vaccine constructs as polymerization of the Fc increases avidity and thus cross-binding to the classical Fcγ receptors expressed on the surface of professional antigen presenting cells [49,50]. In line with this, FcRn mediated sorting of IgG-containing ICs has been shown to enhance cross-presentation to

CD8 + T-cells in CD11b + DC subsets [35], which has been shown to be pivotal for protective CD8 + T-cells responses against colorectal cancer in mice [36].

Using our sensitive ELISA, we were able to measure and compare transport in the presence of both acidic and physiological apical pH environments without the need for labelling of the ligands. Our data show that acidic apical pH, resulted in substantially enhanced FcRn-mediated delivery across polarized cells. The reason for this improvement is most likely a result of FcRn-mediated capture and endocytosis of IgG at or near the cell surface, while uptake under physiological pH conditions is thought to solely rely on fluid phase pinocytosis [42]. Our finding that acidic apical pH results in enhanced FcRn mediated transcellular delivery is also in line with a recent report describing FcRn mediated transepithelial transport of human immunodeficiency virus (HIV)-IgG ICs [92]. Taken together, rational design of Fc-engineered polymeric Fc-fusion molecules together with administration at mucosal sites containing an acidic milieu may be an attractive approach to efficiently deliver therapeutics molecules *via* FcRn.

Finally, increasing evidence suggests that not only the constant Fc part of IgG is important for FcRn binding but that also the Fab region may modulate binding and thus influence the pharmacokinetics [68,69]. One illustrating example is two monoclonal Abs built on human IgG1, ustekinumab and briakinumab (both specific for the p40 subunit of interleukin 12 and 23), which have a median half-life of 22 days and 8–9 days in humans respectively [93–95]. In a recent study, the striking difference in half-life between these monoclonal Abs was explained by differences in charge of their Fab regions that affected dissociation from FcRn through a pH-gradient where briakinumab was shown to be eluted at pH 7.9 while ustekinumab eluted at pH 7.4 [70]. During exocytosis in endothelial cells, FcRn-bound IgG has been shown to be released *via* two pathways, either by complete fusion of the secretory vesicle with the plasma membrane or by a so-called kiss-and-run mechanism where the secretory vesicle remains structurally intact and fuse only partially with the plasma membrane in repetitive cycles [96]. In regard to briakinumab, it has been postulated that its short half-life is due to inefficient release during exocytosis. Interestingly, both charge differences in the complementary determining regions (CDRs) of the Fab as well as the framework of the particular variable heavy and light chains of the Fab have been shown to modulate the pharmacokinetics of Abs [70,97,98]. In this study we showed that removal of the Fab arms of rituximab did not alter the transcellular transport capacity. However, to fully understand the influence of charge differences in CDRs and frameworks between different IgG molecules, a thorough side-by-side comparison of the transport properties of such Abs are needed. The *in vitro* T84 cellular assay described here may thus be a cost efficient way to screen for the ability of IgG molecules and novel fusion formats to be delivered across a monolayer of human epithelial cells prior to *in vivo* studies.

Supplementary data to this article can be found online at http://dx.doi.org/10.1016/j.jconrel.2015.12.033.

Acknowledegments

We are grateful to Sathiaruby Sivaganesh for excellent technical assistance. We also are thankful to Gregory Christianson and Derry Roopenian (The Jackson Laboratory) for providing the ADM31 Ab. This work was supported in part by the Research Council of Norway through its Center of Excellence funding scheme (project number 179573). J.T.A. was supported by the Research Council of Norway (Grant nos. 230526/F20 and 179573/V40). S.F., A.G. and K.M.K.S. were supported by the University of Oslo. M.B. was supported by the Research Council of Norway through its programme for Global Health and Vaccination Research (GLOBVAC) (Grant no. 143822). RP and PB thank the LSTM's Research Centre for Drugs & Diagnostics for providing a Welcome Trust ISSF award that facilitated this study.

References

[1] E.J. Israel, S. Taylor, Z. Wu, E. Mizoguchi, R.S. Blumberg, A. Bhan, et al., Expression of the neonatal Fc receptor, FcRn, on human intestinal epithelial cells, Immunology 92 (1) (1997) 69–74.
[2] G.M. Spiekermann, P.W. Finn, E.S. Ward, J. Dumont, B.L. Dickinson, R.S. Blumberg, et al., Receptor-mediated immunoglobulin G transport across mucosal barriers in adult life: functional expression of FcRn in the mammalian lung, J. Exp. Med. 196 (3) (2002) 303–310.
[3] Z. Li, S. Palaniyandi, R. Zeng, W. Tuo, D.C. Roopenian, X. Zhu, Transfer of IgG in the female genital tract by MHC class I-related neonatal Fc receptor (FcRn) confers protective immunity to vaginal infection, Proc. Natl. Acad. Sci. U. S. A. 108 (11) (2011) 4388–4393.
[4] M. Yoshida, A. Masuda, T.T. Kuo, K. Kobayashi, S.M. Claypool, T. Takagawa, et al., IgG transport across mucosal barriers by neonatal Fc receptor for IgG and mucosal immunity, Springer Semin. Immunopathol. 28 (4) (2006) 397–403.
[5] D.E. Vaughn, P.J. Bjorkman, Structural basis of pH-dependent antibody binding by the neonatal Fc receptor, Structure 6 (1) (1998) 63–73.
[6] M. Raghavan, V.R. Bonagura, S.L. Morrison, P.J. Bjorkman, Analysis of the pH dependence of the neonatal Fc receptor/immunoglobulin G interaction using antibody and receptor variants, Biochemistry 34 (45) (1995) 14649–14657.
[7] N.E. Simister, A.R. Rees, Isolation and characterization of an Fc receptor from neonatal rat small intestine, Eur. J. Immunol. 15 (7) (1985) 733–738.
[8] V. Ghetie, E.S. Ward, Transcytosis and catabolism of antibody, Immunol. Res. 25 (2) (2002) 97–113.
[9] P. Brandtzaeg, Secretory IgA: designed for anti-microbial defense, Front. Immunol. 4 (2013) 222.
[10] K.M. McCarthy, Y. Yoong, N.E. Simister, Bidirectional transcytosis of IgG by the rat neonatal Fc receptor expressed in a rat kidney cell line: a system to study protein transport across epithelia, J. Cell Sci. 113 (Pt 7) (2000) 1277–1285.
[11] A. Praetor, I. Ellinger, W. Hunziker, Intracellular traffic of the MHC class I-like IgG Fc receptor, FcRn, expressed in epithelial MDCK cells, J. Cell Sci. 112 (Pt 14) (1999) 2291–2299.
[12] B.L. Dickinson, K. Badizadegan, Z. Wu, J.C. Ahouse, X. Zhu, N.E. Simister, et al., Bidirectional FcRn-dependent IgG transport in a polarized human intestinal epithelial cell line, J. Clin. Invest. 104 (7) (1999) 903–911.
[13] N.M. Stapleton, J.T. Andersen, A.M. Stemerding, S.P. Bjarnarson, R.C. Verheul, J. Gerritsen, et al., Competition for FcRn-mediated transport gives rise to short half-life of human IgG3 and offers therapeutic potential, Nat. Commun. 2 (2011) 599.
[14] I. Ellinger, M. Schwab, A. Stefanescu, W. Hunziker, R. Fuchs, IgG transport across trophoblast-derived BeWo cells: a model system to study IgG transport in the placenta, Eur. J. Immunol. 29 (3) (1999) 733–744.
[15] P.J. Hornby, P.R. Cooper, C. Kliwinski, E. Ragwan, J.R. Mabus, B. Harman, et al., Human and non-human primate intestinal FcRn expression and immunoglobulin G transcytosis, Pharm. Res. 31 (4) (2014) 908–922.
[16] S.M. Claypool, B.L. Dickinson, M. Yoshida, W.I. Lencer, R.S. Blumberg, Functional reconstitution of human FcRn in Madin–Darby canine kidney cells requires co-expressed human beta 2-microglobulin, J. Biol. Chem. 277 (31) (2002) 28038–28050.
[17] S. Tzaban, R.H. Massol, E. Yen, W. Hamman, S.R. Frank, L.A. Lapierre, et al., The recycling and transcytotic pathways for IgG transport by FcRn are distinct and display an inherent polarity, J. Cell Biol. 185 (4) (2009) 673–684.
[18] C. Medesan, C. Radu, J.K. Kim, V. Ghetie, E.S. Ward, Localization of the site of the IgG molecule that regulates maternofetal transmission in mice, Eur. J. Immunol. 26 (10) (1996) 2533–2536.
[19] M. Yoshida, K. Kobayashi, T.T. Kuo, L. Bry, J.N. Glickman, S.M. Claypool, et al., Neonatal Fc receptor for IgG regulates mucosal immune responses to luminal bacteria, J. Clin. Invest. 116 (8) (2006) 2142–2151.
[20] J.A. Dumont, A.J. Bitonti, D. Clark, S. Evans, M. Pickford, S.P. Newman, Delivery of an erythropoietin-Fc fusion protein by inhalation in humans through an immunoglobulin transport pathway, J. Aerosol Med. 18 (3) (2005) 294–303.
[21] A.J. Bitonti, J.A. Dumont, S.C. Low, R.T. Peters, K.E. Kropp, V.J. Palombella, et al., Pulmonary delivery of an erythropoietin Fc fusion protein in non-human primates through an immunoglobulin transport pathway, Proc. Natl. Acad. Sci. U. S. A. 101 (26) (2004) 9763–9768.
[22] L. Ye, R. Zeng, Y. Bai, D.C. Roopenian, X. Zhu, Efficient mucosal vaccination mediated by the neonatal Fc receptor, Nat. Biotechnol. 29 (2) (2011) 158–163.
[23] L. Lu, S. Palaniyandi, R. Zeng, Y. Bai, X. Liu, Y. Wang, et al., A neonatal Fc receptor-targeted mucosal vaccine strategy effectively induces HIV-1 antigen-specific immunity to genital infection, J. Virol. 85 (20) (2011) 10542–10553.
[24] M. Firan, R. Bawdon, C. Radu, R.J. Ober, D. Eaken, F. Antohe, et al., The MHC class I-related receptor, FcRn, plays an essential role in the maternofetal transfer of gamma-globulin in humans, Int. Immunol. 13 (8) (2001) 993–1002.
[25] L. Mathiesen, L.K. Nielsen, J.T. Andersen, A. Grevys, I. Sandlie, T.E. Michaelsen, et al., Maternofetal transplacental transport of recombinant IgG antibodies lacking effector functions, Blood 122 (7) (2013) 1174–1181.
[26] M. Robert-Guroff, IgG surfaces as an important component in mucosal protection, Nat. Med. 6 (2) (2000) 129–130.
[27] R. Weltzin, T.P. Monath, Intranasal antibody prophylaxis for protection against viral disease, Clin. Microbiol. Rev. 12 (3) (1999) 383–393.
[28] W.W. Merrill, G.P. Naegel, J.J. Olchowski, H.Y. Reynolds, Immunoglobulin G subclass proteins in serum and lavage fluid of normal subjects. Quantitation and comparison with immunoglobulins A and E, Am. Rev. Respir. Dis. 131 (4) (1985) 584–587.
[29] R. Kitz, P. Ahrens, S. Zielen, Immunoglobulin levels in bronchoalveolar lavage fluid of children with chronic chest disease, Pediatr. Pulmonol. 29 (6) (2000) 443–451.

[30] P.A. Kozlowski, S. Cu-Uvin, M.R. Neutra, T.P. Flanigan, Comparison of the oral, rectal, and vaginal immunization routes for induction of antibodies in rectal and genital tract secretions of women, Infect. Immun. 65 (4) (1997) 1387–1394.
[31] T.W. Baba, V. Liska, R. Hofmann-Lehmann, J. Vlasak, W. Xu, S. Ayehunie, et al., Human neutralizing monoclonal antibodies of the IgG1 subtype protect against mucosal simian-human immunodeficiency virus infection, Nat. Med. 6 (2) (2000) 200–206.
[32] J.R. Groothuis, E.A. Simoes, M.J. Levin, C.B. Hall, C.E. Long, W.J. Rodriguez, et al., Prophylactic administration of respiratory syncytial virus immune globulin to high-risk infants and young children. The respiratory syncytial virus immune globulin study group, N. Engl. J. Med. 329 (21) (1993) 1524–1530.
[33] J.R. Mascola, G. Stiegler, T.C. VanCott, H. Katinger, C.B. Carpenter, C.E. Hanson, et al., Protection of macaques against vaginal transmission of a pathogenic HIV-1/SIV chimeric virus by passive infusion of neutralizing antibodies, Nat. Med. 6 (2) (2000) 207–210.
[34] M. Yoshida, S.M. Claypool, J.S. Wagner, E. Mizoguchi, A. Mizoguchi, D.C. Roopenian, et al., Human neonatal Fc receptor mediates transport of IgG into luminal secretions for delivery of antigens to mucosal dendritic cells, Immunity 20 (6) (2004) 769–783.
[35] K. Baker, S.W. Qiao, T.T. Kuo, V.G. Aveson, B. Platzer, J.T. Andersen, et al., Neonatal Fc receptor for IgG (FcRn) regulates cross-presentation of IgG immune complexes by CD8-CD11b + dendritic cells, Proc. Natl. Acad. Sci. U. S. A. 108 (24) (2011) 9927–9932.
[36] K. Baker, T. Rath, M.B. Flak, J.C. Arthur, Z. Chen, J.N. Glickman, et al., Neonatal Fc receptor expression in dendritic cells mediates protective immunity against colorectal cancer, Immunity 39 (6) (2013) 1095–1107.
[37] N. Zarate, S.D. Mohammed, E. O'Shaughnessy, M. Newell, E. Yazaki, N.S. Williams, et al., Accurate localization of a fall in pH within the ileocecal region: validation using a dual-scintigraphic technique, Am. J. Physiol. Gastrointest. Liver Physiol. 299 (6) (2010) G1276–G1286.
[38] M. Koziolek, M. Grimm, D. Becker, V. Iordanov, H. Zou, J. Shimizu, et al., Investigation of pH and temperature profiles in the GI tract of fasted human subjects using the intellicap system, J. Pharm. Sci. (2014).
[39] J.C. Caillouette, C.F. Sharp Jr., G.J. Zimmerman, S. Roy, Vaginal pH as a marker for bacterial pathogens and menopausal status, Am. J. Obstet. Gynecol. 176 (6) (1997) 1270–1275 (discussion 5-7).
[40] J. Atashili, C. Poole, P.M. Ndumbe, A.A. Adimora, J.S. Smith, Bacterial vaginosis and HIV acquisition: a meta-analysis of published studies, AIDS 22 (12) (2008) 1493–1501.
[41] W.A. Hoogerwerf, S.C. Tsao, O. Devuyst, S.A. Levine, C.H. Yun, J.W. Yip, et al., NHE2 and NHE3 are human and rabbit intestinal brush-border proteins, Am. J. Physiol. 270 (1 Pt 1) (1996) G29–G41.
[42] E.S. Ward, R.J. Ober, Commentary: "there's been a flaw in our thinking", Front. Immunol. 6 (2015) 351.
[43] D. Vllasaliu, C. Alexander, M. Garnett, M. Eaton, S. Stolnik, Fc-mediated transport of nanoparticles across airway epithelial cell layers, J. Control. Release 158 (3) (2012) 479–486.
[44] E.M. Pridgen, F. Alexis, T.T. Kuo, E. Levy-Nissenbaum, R. Karnik, R.S. Blumberg, et al., Transepithelial transport of Fc-targeted nanoparticles by the neonatal fc receptor for oral delivery, Sci. Transl. Med. 5 (213) (2013) 213ra167.
[45] L. Guilleminault, N. Azzopardi, C. Arnoult, J. Sobilo, V. Herve, J. Montharu, et al., Fate of inhaled monoclonal antibodies after the deposition of aerosolized particles in the respiratory system, J. Control. Release 196 (2014) 344–354.
[46] A.C. Chan, P.J. Carter, Therapeutic antibodies for autoimmunity and inflammation, Nat. Rev. Immunol. 10 (5) (2010) 301–316.
[47] Y. Wang, Z. Tian, D. Thirumalai, X. Zhang, Neonatal Fc receptor (FcRn): a novel target for therapeutic antibodies and antibody engineering, J. Drug Target. 22 (4) (2014) 269–278.
[48] E.S. Ward, S.C. Devanaboyina, R.J. Ober, Targeting FcRn for the modulation of antibody dynamics, Mol. Immunol. (2015).
[49] D.M. Czajkowsky, J.T. Andersen, A. Fuchs, T.J. Wilson, D. Mekhaiel, M. Colonna, et al., Developing the IVIG biomimetic, hexa-Fc, for drug and vaccine applications, Sci. Rep. 5 (2015) 9526.
[50] D.N. Mekhaiel, D.M. Czajkowsky, J.T. Andersen, J. Shi, M. El-Faham, M. Doenhoff, et al., Polymeric human Fc-fusion proteins with modified effector functions, Sci. Rep. 1 (2011) 124.
[51] L. Norderhaug, T. Olafsen, T.E. Michaelsen, I. Sandlie, Versatile vectors for transient and stable expression of recombinant antibody molecules in mammalian cells, J. Immunol. Methods 204 (1) (1997) 77–87.
[52] A. Grevys, M. Bern, S. Foss, D.B. Bratlie, A. Moen, K.S. Gunnarsen, et al., Fc engineering of human IgG1 for altered binding to the neonatal Fc receptor affects Fc effector functions, J. Immunol. 194 (11) (2015) 5497–5508.
[53] S.W. Qiao, K. Kobayashi, F.E. Johansen, L.M. Sollid, J.T. Andersen, E. Milford, et al., Dependence of antibody-mediated presentation of antigen on FcRn, Proc. Natl. Acad. Sci. U. S. A. 105 (27) (2008) 9337–9342.
[54] S. Popov, J.G. Hubbard, J. Kim, B. Ober, V. Ghetie, E.S. Ward, The stoichiometry and affinity of the interaction of murine Fc fragments with the MHC class I-related receptor, FcRn, Mol. Immunol. 33 (6) (1996) 521–530.
[55] J.T. Andersen, S. Justesen, B. Fleckenstein, T.E. Michaelsen, G. Berntzen, V.E. Kenanova, et al., Ligand binding and antigenic properties of a human neonatal Fc receptor with mutation of two unpaired cysteine residues, FEBS J. 275 (16) (2008) 4097–4110.
[56] G. Berntzen, E. Lunde, M. Flobakk, J.T. Andersen, V. Lauvrak, I. Sandlie, Prolonged and increased expression of soluble Fc receptors, IgG and a TCR-Ig fusion protein by transiently transfected adherent 293E cells, J. Immunol. Methods 298 (1–2) (2005) 93–104.
[57] G.J. Christianson, V.Z. Sun, S. Akilesh, E. Pesavento, G. Proetzel, D.C. Roopenian, Monoclonal antibodies directed against human FcRn and their applications, mAbs 4 (2) (2012) 208–216.
[58] F.H. Niesen, H. Berglund, M. Vedadi, The use of differential scanning fluorimetry to detect ligand interactions that promote protein stability, Nat. Protoc. 2 (9) (2007) 2212–2221.
[59] X. Zhu, G. Meng, B.L. Dickinson, X. Li, E. Mizoguchi, L. Miao, et al., MHC class I-related neonatal Fc receptor for IgG is functionally expressed in monocytes, intestinal macrophages, and dendritic cells, J. Immunol. 166 (5) (2001) 3266–3276.
[60] T. Takizawa, C.L. Anderson, J.M. Robinson, A novel Fc gamma R-defined, IgG-containing organelle in placental endothelium, J. Immunol. 175 (4) (2005) 2331–2339.
[61] R.M. Hershberg, P.E. Framson, D.H. Cho, L.Y. Lee, S. Kovats, J. Beitz, et al., Intestinal epithelial cells use two distinct pathways for HLA class II antigen processing, J. Clin. Invest. 100 (1) (1997) 204–215.
[62] L. Ye, X. Liu, S.N. Rout, Z. Li, Y. Yan, L. Lu, et al., The MHC class II-associated invariant chain interacts with the neonatal Fc gamma receptor and modulates its trafficking to endosomal/lysosomal compartments, J. Immunol. 181 (4) (2008) 2572–2585.
[63] M. Strubin, C. Berte, B. Mach, Alternative splicing and alternative initiation of translation explain the four forms of the Ia antigen-associated invariant chain, EMBO J. 5 (13) (1986) 3483–3488.
[64] K.M. Sand, B. Dalhus, G.J. Christianson, M. Bern, S. Foss, J. Cameron, et al., Dissection of the neonatal Fc receptor (FcRn)-albumin interface using mutagenesis and anti-FcRn albumin-blocking antibodies, J. Biol. Chem. 289 (24) (2014) 17228–17239.
[65] S.M. Claypool, B.L. Dickinson, J.S. Wagner, F.E. Johansen, N. Venu, J.A. Borawski, et al., Bidirectional transepithelial IgG transport by a strongly polarized basolateral membrane fcgamma-receptor, Mol. Biol. Cell 15 (4) (2004) 1746–1759.
[66] T. Yoshimori, A. Yamamoto, Y. Moriyama, M. Futai, Y. Tashiro, Bafilomycin A1, a specific inhibitor of vacuolar-type H(+)-ATPase, inhibits acidification and protein degradation in lysosomes of cultured cells, J. Biol. Chem. 266 (26) (1991) 17707–17712.
[67] A.S. De Groot, D.W. Scott, Immunogenicity of protein therapeutics, Trends Immunol. 28 (11) (2007) 482–490.
[68] T. Schlothauer, P. Rueger, J.O. Stracke, H. Hertenberger, F. Fingas, L. Kling, et al., Analytical FcRn affinity chromatography for functional characterization of monoclonal antibodies, mAbs 5 (4) (2013) 576–586.
[69] W. Wang, P. Lu, Y. Fang, L. Hamuro, T. Pittman, B. Carr, et al., Monoclonal antibodies with identical Fc sequences can bind to FcRn differentially with pharmacokinetic consequences, Drug Metab. Dispos. 39 (9) (2011) 1469–1477.
[70] A. Schoch, H. Kettenberger, O. Mundigl, G. Winter, J. Engert, J. Heinrich, et al., Charge-mediated influence of the antibody variable domain on FcRn-dependent pharmacokinetics, Proc. Natl. Acad. Sci. U. S. A. 112 (19) (2015) 5997–6002.
[71] P.F. Jensen, V. Larraillet, T. Schlothauer, H. Kettenberger, M. Hilger, K.D. Rand, Investigating the interaction between the neonatal Fc receptor and monoclonal antibody variants by hydrogen/deuterium exchange mass spectrometry, Mol. Cell. Proteomics 14 (1) (2015) 148–161.
[72] H.P. Montoyo, C. Vaccaro, M. Hafner, R.J. Ober, W. Mueller, E.S. Ward, Conditional deletion of the MHC class I-related receptor FcRn reveals the sites of IgG homeostasis in mice, Proc. Natl. Acad. Sci. U. S. A. 106 (8) (2009) 2788–2793.
[73] A. Morell, W.D. Terry, T.A. Waldmann, Metabolic properties of IgG subclasses in man, J. Clin. Invest. 49 (4) (1970) 673–680.
[74] W.F. Dall'Acqua, P.A. Kiener, H. Wu, Properties of human IgG1s engineered for enhanced binding to the neonatal Fc receptor (FcRn), J. Biol. Chem. 281 (33) (2006) 23514–23524.
[75] J. Zalevsky, A.K. Chamberlain, H.M. Horton, S. Karki, I.W. Leung, T.J. Sproule, et al., Enhanced antibody half-life improves in vivo activity, Nat. Biotechnol. 28 (2) (2010) 157–159.
[76] C. Vaccaro, R. Bawdon, S. Wanjie, R.J. Ober, E.S. Ward, Divergent activities of an engineered antibody in murine and human systems have implications for therapeutic antibodies, Proc. Natl. Acad. Sci. U. S. A. 103 (49) (2006) 18709–18714.
[77] M.J. Borrok, Y. Wu, N. Beyaz, X.Q. Yu, V. Oganesyan, W.F. Dall'Acqua, et al., pH-dependent binding engineering reveals an FcRn affinity threshold that governs IgG recycling, J. Biol. Chem. 290 (7) (2015) 4282–4290.
[78] G.J. Robbie, R. Criste, W.F. Dall'acqua, K. Jensen, N.K. Patel, G.A. Losonsky, et al., A novel investigational Fc-modified humanized monoclonal antibody, motavizumab-YTE, has an extended half-life in healthy adults, Antimicrob. Agents Chemother. 57 (12) (2013) 6147–6153.
[79] C. Vaccaro, J. Zhou, R.J. Ober, E.S. Ward, Engineering the Fc region of immunoglobulin G to modulate in vivo antibody levels, Nat. Biotechnol. 23 (10) (2005) 1283–1288.
[80] D.A. Patel, A. Puig-Canto, D.K. Challa, H. Perez Montoyo, R.J. Ober, E.S. Ward, Neonatal Fc receptor blockade by Fc engineering ameliorates arthritis in a murine model, J. Immunol. 187 (2) (2011) 1015–1022.
[81] D.K. Challa, U. Bussmeyer, T. Khan, H.P. Montoyo, P. Bansal, R.J. Ober, et al., Autoantibody depletion ameliorates disease in murine experimental autoimmune encephalomyelitis, mAbs 5 (5) (2013) 655–659.
[82] W. He, M.S. Ladinsky, K.E. Huey-Tubman, G.J. Jensen, J.R. McIntosh, P.J. Bjorkman, FcRn-mediated antibody transport across epithelial cells revealed by electron tomography, Nature 455 (7212) (2008) 542–546.
[83] T. Rath, K. Baker, J.A. Dumont, R.T. Peters, H. Jiang, S.W. Qiao, et al., Fc-fusion proteins and FcRn: structural insights for longer-lasting and more effective therapeutics, Crit. Rev. Biotechnol. 35 (2) (2015) 235–254.
[84] D.M. Czajkowsky, J. Hu, Z. Shao, R.J. Pleass, Fc-fusion proteins: new developments and future perspectives, EMBO Mol. Med. 4 (10) (2012) 1015–1028.
[85] J.T. Andersen, S. Foss, V.E. Kenanova, T. Olafsen, I.S. Leikfoss, D.C. Roopenian, et al., Anti-carcinoembryonic antigen single-chain variable fragment antibody variants bind mouse and human neonatal Fc receptor with different affinities that reveal distinct cross-species differences in serum half-life, J. Biol. Chem. 287 (27) (2012) 22927–22937.

[86] J.K. Kim, M. Firan, C.G. Radu, C.H. Kim, V. Ghetie, E.S. Ward, Mapping the site on human IgG for binding of the MHC class I-related receptor, FcRn, Eur. J. Immunol. 29 (9) (1999) 2819–2825.
[87] S.Y. Ko, A. Pegu, R.S. Rudicell, Z.Y. Yang, M.G. Joyce, X. Chen, et al., Enhanced neonatal Fc receptor function improves protection against primate SHIV infection, Nature 514 (7524) (2014) 642–645.
[88] M.J. Bernett, S.Y. Chu, I. Leung, G.L. Moore, S.H. Lee, E. Pong, et al., Immune suppression in cynomolgus monkeys by XPro9523: an improved CTLA4-Ig fusion with enhanced binding to CD80, CD86 and neonatal Fc receptor FcRn, mAbs 5 (3) (2013) 384–396.
[89] E.S. Ward, S.C. Devanaboyina, R.J. Ober, Targeting FcRn for the modulation of antibody dynamics, Mol. Immunol. 67 (2 Pt A) (2015) 131–141.
[90] A.W. Weflen, N. Baier, Q.J. Tang, M. Van den Hof, R.S. Blumberg, W.I. Lencer, et al., Multivalent immune complexes divert FcRn to lysosomes by exclusion from recycling sorting tubules, Mol. Biol. Cell 24 (15) (2013) 2398–2405.
[91] T. Dashivets, M. Thomann, P. Rueger, A. Knaupp, J. Buchner, T. Schlothauer, Multi-angle effector function analysis of human monoclonal IgG glycovariants, PLoS ONE 10 (12) (2015) e0143520.
[92] S. Gupta, J.S. Gach, J.C. Becerra, T.B. Phan, J. Pudney, Z. Moldoveanu, et al., The neonatal Fc receptor (FcRn) enhances human immunodeficiency virus type 1 (HIV-1) transcytosis across epithelial cells, PLoS Pathog. 9 (11) (2013) e1003776.
[93] M. Gandhi, E. Alwawi, K.B. Gordon, Anti-p40 antibodies ustekinumab and briakinumab: blockade of interleukin-12 and interleukin-23 in the treatment of psoriasis, Semin. Cutan. Med. Surg. 29 (1) (2010) 48–52.
[94] X.T. Lima, K. Abuabara, A.B. Kimball, H.C. Lima, Briakinumab, Expert. Opin. Biol. Ther. 9 (8) (2009) 1107–1113.
[95] W. Weger, Current status and new developments in the treatment of psoriasis and psoriatic arthritis with biological agents, Br. J. Pharmacol. 160 (4) (2010) 810–820.
[96] R.J. Ober, C. Martinez, X. Lai, J. Zhou, E.S. Ward, Exocytosis of IgG as mediated by the receptor, FcRn: an analysis at the single-molecule level, Proc. Natl. Acad. Sci. U. S. A. 101 (30) (2004) 11076–11081.
[97] B. Li, D. Tesar, C.A. Boswell, H.S. Cahaya, A. Wong, J. Zhang, et al., Framework selection can influence pharmacokinetics of a humanized therapeutic antibody through differences in molecule charge, mAbs 6 (5) (2014) 1255–1264.
[98] T. Igawa, H. Tsunoda, T. Tachibana, A. Maeda, F. Mimoto, C. Moriyama, et al., Reduced elimination of IgG antibodies by engineering the variable region, Protein Eng. Des. Sel. 23 (5) (2010) 385–392.
[99] E.O. Saphire, P.W. Parren, R. Pantophlet, M.B. Zwick, G.M. Morris, P.M. Rudd, et al., Crystal structure of a neutralizing human IGG against HIV-1: a template for vaccine design, Science 293 (5532) (2001) 1155–1159.